

Numerical solution of the bivariate population balance equation for the interacting hydrodynamics and mass transfer in liquid–liquid extraction columns

Menwer M. Attarakih^a, Hans-Jörg Bart^{a,*}, Naim M. Faqir^b

^a*Faculty of Mechanical and Process Engineering, Institute of Thermal Process Engineering, University of Kaiserslautern, POB 3049, D-67653 Kaiserslautern, Germany*

^b*Faculty of Engineering and Technology, Chemical Engineering Department, University of Jordan, 11942 Amman, Jordan*

Received 1 June 2004; accepted 1 December 2004

Available online 22 June 2005

Abstract

A comprehensive model for predicting the interacting hydrodynamics and mass transfer is formulated on the basis of a spatially distributed population balance equation in terms of the bivariate number density function with respect to droplet diameter and solute concentration. The two macro- (droplet breakage and coalescence) and micro- (interphase mass transfer) droplet phenomena are allowed to interact through the dispersion interfacial tension. The resulting model equations are composed of a system of partial and algebraic equations that are dominated by convection, and hence it calls for a specialized discretization approach. The model equations are applied to a laboratory segment of an RDC column using an experimentally validated droplet transport and interaction functions. Aside from the model spatial discretization, two methods for the discretization of the droplet diameter are extended to include the droplet solute concentration. These methods are the generalized fixed-pivot technique (GFP) and the quadrature method of moments (QMOM). The numerical results obtained from the two extended methods are almost identical, and the CPU time of both methods is found acceptable so that the two methods are being extended to simulate a full-scale liquid–liquid extraction column.

© 2005 Elsevier Ltd. All rights reserved.

Keywords: Population balance; Breakage; Coalescence; Hydrodynamics; Mass transfer; Simulation

1. Introduction

The liquid–liquid extraction columns (LLECs) are one of the major multiphase contacting equipment that received a wide industrial acceptance in many fields of engineering such as hydrometallurgical, nuclear, petrochemical, pharmaceutical and food industries. However, the optimal design of such equipment has not yet been fulfilled and still dependent on the time-consuming and expensive scale-up

methods from the laboratory scale pilot plants. This is due to the complex nature of the macroscopic dispersed phase interactions as well as the microscopic interphase mass transfer occurring in the continuously turbulent flow field. These macroscopic interactions such as droplet breakage and coalescence coupled to the interphase mass transfer result in a distributed population of droplets. This population is not only distributed in the spatial domain of the contacting equipment, but also randomly distributed with respect to the droplet state (properties) such as size, concentration and age. The hydrodynamic and mass transfer interactions could be simulated using the population balances as an effective framework taking into account the bivariate nature (with respect to droplet size and concentration) of the spatially distributed

* Corresponding author. Tel.: +49 631 205 24 14; fax: +49 631 205 21 19.
E-mail address: bart@mv.uni-kl.de (H.-J. Bart)
URL: <http://www.uni-kl.de/LS-Bart/> (H.-J. Bart).

populations in the interacting liquid–liquid dispersions. So, in contrast to the previous spatially distributed population balance equation (SDPBE) describing the performance of the LLECs (Mohanty, 2000; Bart, 2003), this modeling approach allows the dynamic interaction of the mass transfer and fluid hydrodynamics by leaving it open to introduce a suitable model for predicting the interfacial tension, which changes with the mass transfer and markedly affects the breakage and coalescence rates (Gourdon et al., 1994). In the present work, the state of any droplet is represented by a bivariate (joint) density function $n_{d,c_y}(d, c_y; t, z)$, where $n_{d,c_y}(d, c_y; t, z) \partial d \partial c_y$ represents the number of droplets having size and concentration in the ranges $[d \pm \delta d]$ and $[c_y \pm \delta c_y]$ per unit volume of the reactor. This allows the discontinuous macroscopic (breakage and coalescence) and the continuous microscopic (interphase mass transfer) events to be coupled in a single SDPBE along with the transport equations describing the hydrodynamics and mass transfer of the continuous phase. These equations represent a system of mixed integro-partial and algebraic equations for which no analytical solution exists except for strongly simplified forms, and hence a numerical solution is required in general. There is a huge published literature to solve the spatially homogenous PBEs, where recent reviews could be found in Ramkrishna (2000) and Attarakih et al. (2004a). These methods could be classified into zero and higher-order methods, where the zero order methods represent the number density function by a constant value in contiguous intervals Kostoglou and Karabelas (1994). On the other hand, the higher-order methods approximate the number density function by a higher-order polynomial, usually of degree three, on finite elements or continuous polynomials (Hamilton et al., 2003; Nicmanis and Hounslow, 1998). An important subgroup of the zero-order methods is the so-called internally consistent methods with respect to selected integral properties. By internal consistency it is meant that the desired integral property associated with the average number density obtained from the discrete PBE should be the same as that obtained from its continuous counterpart (Ramkrishna, 2000). This internal consistency is found to predict accurately the desired integral properties, and at the same time improves the accuracy of the predicted droplet distribution on coarse grids (Ramkrishna, 2000). Attarakih et al. (2004a) extended the fixed-pivot technique of Kumar and Ramkrishna (1996) to continuous flow systems; particularly, to describe the hydrodynamics of an RDC LLEC. The extended scheme is called the generalized fixed-pivot (GFP) technique and is found sufficiently fast to simulate the hydrodynamic behavior of the aforementioned LLEC.

An alternative way for solving the PBE is through the use of the method of moments (MOM), where the dimensionality of the PBE with respect to the internal coordinates is reduced by integrating all or some of them. As pointed out by Hulburt and Katz (1964), the MOM suffers from closure problems; that is, the difficulty of expressing the PBE in terms of a complete and finite set of moments. This prob-

lem is recently addressed and reviewed by Diemer and Olson (2002). Kostoglou and Karabelas (2002) assessed many variants of the MOM for solving the PBE for droplet breakage in a batch vessel. They concluded that the interpolative closure rule, based on the Lagrange polynomials using the logarithm of the moments as the dependent variable and the moments index as the independent one, is a sufficiently accurate approach.

A general and sufficiently accurate approach to overcome the aforementioned closure problem is introduced by McGraw (1997) and is called the quadrature method of moments (QMOM). The method is based on the work of Gordon (1968) where he reformulated the problem of Gauss-type integration with respect to any arbitrary weight function. Instead of the high-order polynomials used to find the Gauss quadrature weights and abscissas, the approach of Gordon (1968) is to make use of the low-order moments of the distribution to find these weights and abscissas by solving a well-conditioned eigenvalue problem. The method is found to produce accurate numerical results without any prior knowledge of the number density function or severe simplification of the breakage and coalescence frequencies. The QMOM is extensively tested and validated where it proved to be an efficient method providing a compromise between the full rigor and feasible numerical solutions (Marchisio et al., 2003a,b; McGraw, 1997; McGraw and Wright, 2003; Piskunov and Golubev, 2002; Wright et al., 2001). Most of this published work is concerned with only one internal coordinate (droplet size); however, Wright et al. (2001) were among the first who tried to extend this method to bivariate PBEs. They extended the QMOM (it is called the bivariate quadrature method of moments (BVQMOM)) to simulate inorganic nanoparticles undergoing simultaneous coagulation and sintering. Rosner and Pyykónen (2002) followed the same aforementioned approach and they reported some computational problems concerning the routine (ORTHOG) that finds the quadrature points. Piskunov and Golubev (2002) tried to find the quadrature nodes by expressing them as roots of some polynomial of unknown coefficients. This problem of roots finding is a well-known ill-conditioned problem, especially when the polynomial order is greater than four (Gordon, 1968). They then tried a combination of these polynomial coefficients and the time derivatives of the weights and nodes of the quadrature; however, the problem of the ill-conditioned matrix composed of the time derivative coefficients is inherently involved in the algorithm. In spite of these difficulties, the QMOM represents an attractive approach for solving the PBEs, where their complexity prevents sometimes the direct discretization methods from being easily applied. In this context, the QMOM is being implemented in the commercial CFD codes to solve the multi-phase flow problems (Marchisio et al., 2003a,b; Rosner and Pyykónen, 2002; Rosner et al., 2003).

So, in the present work we adopted the BVQMOM to solve the bivariate SDPBEs describing the coupled hydrodynamics and mass transfer without any simplification of the

breakage and coalescence frequencies or the transport functions related to the droplet motion and axial transport. Additionally, we present a simple reconstruction approach for the marginal densities of the bivariate density function. The performance of the QMOM for solving this bivariate problem is extensively compared to the GFP algorithm developed by the authors (Attarakih et al., 2004a), which is already extended to include mass transfer and is denoted by GFPMT. Due to the space limitation, the GFPMT algorithm will be reported separately in a subsequent publication. Moreover, and for the sake of isolating the spatial discretization errors due to the droplet convection, our focus in this contribution is mainly on the internal coordinate discretization. Accordingly, a four-compartment model of a short segment of the aforementioned RDC column will only be considered. For the spatial discretization, the interested reader could refer to our work found in Attarakih et al. (2004a).

2. The mathematical model

2.1. Hydrodynamics and mass transfer of the dispersed phase

The general SDPBE for describing the coupled hydrodynamics and mass transfer in LLECs in a one-spatial domain could be written as

$$\begin{aligned} \frac{\partial n_{d,c_y}(\psi)}{\partial t} + \frac{\partial [u_y n_{d,c_y}(\psi)]}{\partial z} + \sum_{i=1}^2 \frac{\partial [\dot{\zeta}_i n_{d,c_y}(\psi)]}{\partial \zeta_i} \\ = \frac{\partial}{\partial z} \left[D_y \frac{\partial n_{d,c_y}(\psi)}{\partial z} \right] + \frac{Q_y^{\text{in}}}{A_c} n_y^{\text{in}}(d, c_y; t) \delta(z - z_y) \\ + \mathcal{Y}\{\psi\}. \end{aligned} \quad (1)$$

In this equation, the components of the vector $\psi = [d \ c_y \ z \ t]$ are those for the droplet internal coordinates (diameter and solute concentration), the external coordinate (column height), z , and the time, t , where the velocity vector along the internal coordinates is given by $\dot{\zeta} = [d \ \dot{c}_y]$. The source term $\mathcal{Y}\{\psi\}$ represents the net number of droplets produced by breakage and coalescence per unit volume and unit time in the coordinate range $\zeta \pm \partial\zeta$. The left-hand side is the continuity operator in both the external and internal coordinates, while the first part on the right-hand side is the droplet axial dispersion characterized by the dispersion coefficient, D_y , which might be dependent on the energy dissipation and the droplet rising velocity (Modes, 2000). The second term on the right-hand side is the rate at which the droplets enter the LLEC with volumetric flow rate, Q_y^{in} , that is perpendicular to the column cross-sectional area, A_c , at a location z_y with an inlet number density, n_y^{in} , and is treated as a point source in space. The dispersed phase velocity, u_y , relative to the walls of the column is determined in terms

of the relative (slip) velocity with respect to the continuous phase

$$u_r = u_y - u_x = (1 - \phi_y)u_s, \quad (2)$$

where u_r is written in terms of the velocity, u_s , which is related to the droplet terminal velocity relative to the column walls based on the mass-average velocity of the multiphase mixture (Manninen et al., 1996).

The velocity, u_s , appearing in the above equation could be related to the single droplet terminal velocity, u_t , to take into account the droplet swarm and the flow conditions in a specific equipment:

$$u_s = K_v u_t(d, \mathbf{P}), \quad (3)$$

where \mathbf{P} is a vector of physical properties ($[\mu \ \rho \ \sigma]$) and K_v is a slowing factor taking into account the effect of the column internal geometry on the droplet terminal velocity ($0 < K_v \leq 1$) (Modes, 2000). A useful guide for selecting the suitable droplet terminal velocity based on the shape of the droplet (rigid, oscillating or circulating), and hence on the system physical properties, could be found in Gourdon et al. (1994). In the above equation, the state of local equilibrium is assumed and hence the droplet is considered to accelerate to its terminal velocity in a short time (Manninen et al., 1996).

2.2. Hydrodynamics and mass transfer of the continuous phase

The transport equations describing hydrodynamics and the solute concentration, c_x , in the continuous phase taking into account the interphase mass transfer from the continuous to the dispersed phase could be written as

$$\frac{\partial(\phi_x)}{\partial t} - \frac{\partial}{\partial z} \left(u_x \phi_x + D_x \frac{\partial(\phi_x)}{\partial z} \right) = \frac{Q_x^{\text{in}}}{A_c} \delta(z - z_y), \quad (4)$$

$$\begin{aligned} \frac{\partial(\phi_x c_x)}{\partial t} - \frac{\partial}{\partial z} \left(u_x \phi_x c_x + D_x \frac{\partial(\phi_x c_x)}{\partial z} \right) \\ = \frac{Q_x^{\text{in}} c_x^{\text{in}}}{A_c} \delta(z - z_y) - \int_0^\infty \int_0^{c_y, \text{max}} \dot{c}_y v(d) n_{v,c_y}(\psi) \partial d \partial c_y. \end{aligned} \quad (5)$$

The assumption that is inherent in these two equations is that the density of the continuous phase is approximately constant; that is, the quantity of the solute transferred from the continuous to the dispersed phase is small, which is the usual case. The volume fraction of the continuous phase, ϕ_x , clearly satisfies the physical constraint: $\phi_x + \phi_y = 1$. The left-hand side of Eq. (5) as well as the first term on the right-hand side have the same interpretations as that for Eq. (1), however, with respect to the continuous phase. The last term appearing in Eq. (5) is the total rate of solute transferred from the continuous to the dispersed phase, where the liquid droplets are treated as point sources (Ramkrishna, 2000). Note that Eq. (1) is coupled to the solute balance in the

Table 1

The birth and death terms for the SDPBE in the presence of mass transfer (see Eq. (6))

$$\begin{aligned}
 B^b & \int_d^{d_{\max}} \int_0^{c_{y,\max}} \Gamma(d', \phi_y, \mathbf{P}) \beta_n(d|d') n_{d,c_y}(d', c'_y; t, z) \delta(c'_y - c_y) \partial d' \partial c'_y \\
 D^b & -\Gamma(d, \phi_y, \mathbf{P}) n_{d,c_y}(d, c_y; t, z) \\
 B^c & \frac{1}{2} \int_0^d \int_{c'_{y,\min}}^{c'_{y,\max}} \omega(d', \eta, \phi_y, \mathbf{P}) \left(\frac{d}{\eta}\right)^5 n_{d,c_y}(d', c'_y; t, z) n_{d,c_y}(\eta, c''_y; t, z) \partial d' \partial c'_y, \quad \eta = (d^3 - d'^3)^{1/3}, \quad c''_y = \frac{c_y v(d) - c'_y v(d')}{v(d) - v(d')} \\
 & c'_{y,\min} = \max(0, c_{y,\max}(1 - v(d)/v(d')(1 - c_y/c_{y,\max}))), \quad c'_{y,\max} = \min(c_{y,\max}, (v(d)/v(d'))c_y) \\
 D^c & n_{d,c_y}(d, c_y; t, z) \int_0^{(d_{\max}^3 - d^3)^{1/3}} \int_0^{c_{y,\max}} \omega(d, d', \phi_y, \mathbf{P}) n_{d,c_y}(d', c'_y; t, z) \partial d' \partial c'_y
 \end{aligned}$$

continuous phase given by Eq. (5) through the convective and the source terms.

The continuous phase velocity, u_x , with respect to the column walls is obtained by simultaneously solving the continuity equations of the continuous (Eq. (4)) and the dispersed (Eq. (1)) phases, respectively, and is given by Attarakih et al. (2004a). Moreover, in the above derivation the droplet interaction mechanisms are considered fast when compared to the mass transfer (Ribeiro et al., 1997). This means that the mass transfer is considered to take place only during the droplet motion in the continuous phase and the resulting droplets from either droplet breakage or coalescence are considered to have uniform solute concentrations.

2.3. Breakage and coalescence functions

The source term appearing in Eq. (1) could be expanded as

$$\begin{aligned}
 \Upsilon & = B^b(d, c_y; t, z) - D^b(d, c_y; t, z) + B^c(d, c_y; t, z) \\
 & - D^c(d, c_y; t, z), \quad (6)
 \end{aligned}$$

where B^b and B^c are the rate of droplets birth due to droplet breakage and coalescence, respectively, and D^b and D^c are the rates of droplet loss (death) due to droplet breakage and coalescence, respectively, and are shown in Table 1. Note that the transformation of variables $(d', c'_y) \rightarrow (\eta, c''_y)$ is included in the coalescence birth term, D^b , which is represented by $(d/\eta)^3$.

2.3.1. Breakage functions

To complete the description of the droplet breakage, models for the breakage frequency as well as the daughter droplet distribution (β_n) should be completely defined. For droplet breakage in an RDC column, it is experimentally observed that the droplet breakage is mainly determined by the action of the shearing force resulting from the rotating disk (Cauwenberg et al., 1997; Simon et al., 2003). Cauwenberg et al. (1997) suggested the correlation of the breakage probability (fraction of mother droplets that are broken up) to a

modified Weber number. This takes into account the critical rotor speed below which the shear force imparted to the droplet is considered not enough to exceed its surface energy. As pointed out in Section 1, it is the interfacial tension rather than the other physical properties (viscosity or density) that plays the major role in the droplet breakage. Since the measurement of the non-equilibrium interfacial tension as a function of solute concentration is not yet well established, it is of great importance to include at least the effect of the equilibrium interfacial tension on the droplet breakage.

Recently, Schmidt et al. (2003) studied the effect of the equilibrium solute concentration (acetone) on the interfacial tension, and hence the breakage probability in a segment of an RDC column based on the single-droplet experiments. They found that the breakage probability increases as the equilibrium interfacial tension decreases for the two studied systems (water–acetone–toluene and water–butyl acetate). Within this context they followed Cauwenberg et al. (1997) and correlated the breakage probability using the two aforementioned chemical systems (and hence the expressions of $\Gamma(d, \phi_y, N)$ and $\beta_n(d|d')$).

2.3.2. Coalescence functions

In general, the droplet coalescence is more complex than the droplet breakage since it involves the interaction between two droplets and the intervening liquid film from the continuous phase. The physicochemical properties of this film and the turbulent fluctuations play an important role in droplet coalescence. Coalescence is believed to occur if the random contact time between any two coalescing droplets exceeds the time required for the complete intervening film drainage and rupture (Coulaloglou and Tavlarides, 1977). These authors expressed the coalescence frequency as a product of collision rate and coalescence efficiency based on the kinetic theory of gases with two fitting parameters. In this work, the values of these parameters are estimated on the basis of the hydrodynamic model of Attarakih et al. (2004a) for a short segment of an RDC column of five compartments,

and the experimental data of Simon (2004) for the system toluene–water. Since the direction of mass transfer is from the continuous to the dispersed phase, it is expected that the coalescence efficiency to be close to 0 (Gourdon et al., 1994).

2.4. Mass transfer coefficients

The dispersed phase individual mass transfer coefficient is found dependent on the behavior of the single droplet in the sense whether it is stagnant, circulating or oscillating (Kumar and Hartland, 1999). In the present work, the simplified model of Handlos and Baron (1957) as used by many researches (Zhang et al., 1985; Weinstein et al., 1998) as well as the correlation of Kumar and Hartland (1999) are used. However, the criterion based on the Reynolds number as suggested by Zhang et al. (1985) may be used as a guide for selecting the proper mass transfer model. The individual mass transfer coefficient for the continuous phase is essentially subjected to the aforementioned classification procedure, where two models are used to predict it. The first simple one is based on the film coefficient equation as recommended by Weinstein et al. (1998), and the second one is based on the correlation of Kumar and Hartland (1999) for RDC LLECs.

Now, once the individual mass transfer coefficients are estimated, the rate of change of solute concentration in the liquid droplet (\dot{c}_y) is expressed in terms of the droplet volume average concentration and the overall mass transfer coefficient, K_{oy} :

$$\frac{\partial c_y(z, t)}{\partial t} = \frac{6K_{oy}}{d} (c_y^*(c_x) - c_y(z, t)). \quad (7)$$

Note that K_{oy} may be the function of the droplet diameter, d , and time depending on the internal state of the droplet; that is, whether it is circulating or behaving like a rigid sphere. The overall mass transfer coefficient is usually expressed using the two-resistance theory in terms of the individual mass transfer coefficients for the continuous and the dispersed phases (Ribeiro et al., 1997) and $c_y^* = (\partial c_y / \partial c_x) c_x$.

To complete the mathematical model described above, boundary and initial conditions are required. Concerning the boundary conditions, we adopted those of Wilburn (1964) where the details are found in Attarakih et al. (2004a). The initial conditions are taken as zero dispersed phase hold-up and uniform solute concentration in the continuous phase. The inlet bivariate number density is taken as $n_y^{\text{in}}(d, c_y; t) = n_y^{\text{in}}(d; t) \times c_y^{\text{in}}$, which means that all the inlet droplets have the same uniform solute concentration (zero in the present work).

3. The Bivariate Quadrature Method of Moments (BVQMOM)

The above mathematical model is a mixture of integro-partial differential and algebraic equations, which unfortu-

nately admits no general analytical solution due to the inherent nonlinearity in the convective as well as the source terms. Accordingly, a numerical solution for such important mathematical problem is to be sought. So, in this contribution, we extend the QMOM (McGraw, 1997) for solving the simultaneous hydrodynamics and mass transfer in an LLEC as described by the above mathematical model.

As mentioned in Section 1, the BVQMOM transformed the SDPBE into a set of partial differential and algebraic equations via the two-dimensional moment transformation:

$$\mu_{k,m}(t, z) = \int_0^\infty d^k c_y^m n_{d,c_y}(\psi) \partial d \partial c_y. \quad (8)$$

By applying the above transformation to Eqs. (1), (5) and (6), we get the following moment equations:

$$\begin{aligned} \frac{\partial \mu_{k,m}(t, z)}{\partial t} + \frac{\partial}{\partial z} \left[\bar{F}_{k,m}(t, z) - D_y \frac{\partial \mu_{k,m}(t, z)}{\partial z} \right] \\ = \frac{Q_y^{\text{in}}}{A_c} c_y^{\text{in}} \mu_k^{\text{in}}(t) \delta(z - z_y) + m \int_0^{c_{y,\text{max}}} c_y^{m-1} \dot{c}_y n_{d,c_y} \\ \times (\psi) \partial c_y + \bar{Y}_{k,m}, \end{aligned} \quad (9)$$

$$\begin{aligned} \frac{\partial (\phi_x c_x)}{\partial t} - \frac{\partial}{\partial z} \left(u_x \phi_x c_x + D_x \frac{\partial (\phi_x c_x)}{\partial z} \right) \\ = \frac{Q_x^{\text{in}} c_x^{\text{in}}}{A_c} \delta(z - z_y) - \int_0^\infty \int_0^{c_{y,\text{max}}} \dot{c}_y v(d) n_{d,c_y} \\ \times (\psi) \partial d \partial c_y, \end{aligned} \quad (10)$$

$$\begin{aligned} \bar{Y}_{k,m} = \bar{B}_{k,m}(t, z) + \bar{C}_{k,m}(t, z), \\ k, m = 0, 1, \dots, 2N_q - 1, \end{aligned} \quad (11)$$

$$\bar{F}_{k,m} = \int_0^\infty \int_0^{c_{y,\text{max}}} u_y(d, \phi_y, \mathbf{P}) d^k c_y^m n_{d,c_y}(\psi) \partial d \partial c_y, \quad (12)$$

where N_q is the number of the quadrature points and the elements of the transformed source term are relatively more complex and require lengthy but straightforward algebraic manipulations, which finally lead to the following relations:

$$\begin{aligned} \bar{B}_{k,m}(t, z) = \int_0^\infty \int_0^{c_{y,\text{max}}} \Gamma(d', \phi_y, \mathbf{P}) d'^k c_y'^m n_{d,c_y} \\ \times (\psi) \partial c_y' \partial d' \left(\int_0^{d'} \left[\frac{d}{d'} \right]^k \beta_n(d|d') \partial d - 1 \right), \end{aligned} \quad (13)$$

$$\begin{aligned} \bar{C}_{k,m} = \int_0^\infty \int_0^\infty q_m(d'; t, z) n_d(d; t, z) \\ \times (d'^3 (d^3 + d'^3)^{(k-3)/3} - d'^k) \partial d \partial d', \end{aligned} \quad (14)$$

where q_m is given by

$$q_m(d'; t, z) = \int_0^{c_{y,\text{max}}} \omega(d, d', \phi_y, \mathbf{P}) c_y^m n_{d,c_y}(\psi) \partial c_y. \quad (15)$$

The above system of equations could not be solved in its present form for $\mu_{k,m}$ since the source terms due to droplet breakage and coalescence (Eqs. (13) and (14), respectively)

and those describing the droplet convection along the internal (the second two terms of the right-hand side in Eqs. (9) and (10)) and the external coordinates (Eq. (12)) involve the unknown bivariate density function, $n_{d,c_y}(\psi)$. This system of equations is said to be unclosed since the terms involving integrals over the bivariate density, $n_{d,c_y}(\psi)$, cannot be expressed in terms of the moments $\mu_{k,m}$. A general closure rule that circumvents this problem is introduced by Gordon (1968) to evaluate integrals over a distribution of one internal coordinate using a Gauss-type integration with respect to an arbitrary weight function. Following these lines the bivariate density function, $n_{d,c_y}(\psi)$, could be approximated by

$$n_{d,c_y}(\psi) = \sum_{j=1}^{N_q} \sum_{n=1}^{N_q} w_{j,n} \delta(d - d_j) \delta(c_y - c_{y,n}), \quad (16)$$

where the strength (weights) and location of the Dirac delta function (abscissa) are determined on the basis of knowledge of the low-order moments ($\mu_{k,m}$, $k, m=0, 1, \dots, 2N_q-1$). The substitution of Eq. (16) in the unclosed terms of Eqs. (9)–(15) results in a system of PDEs in space and time in addition to the following system of algebraic equations resulting from the combination of Eqs. (8) and (16):

$$\mu_{k,m}(t, z) = \sum_{j=1}^{N_q} \sum_{n=1}^{N_q} w_{j,n} d_j^k c_{y,n}^m. \quad (17)$$

Now, the solution methodology proceeds by first splitting Eqs. (9)–(15) into two coupled systems of spatially distributed moment equations in terms of the bivariate moments:

$$\mu_{k,0}(t, z) = \sum_{j=1}^{N_q} w_{j,1} d_j^k, \quad (18)$$

$$\mu_{k,1}(t, z) = \sum_{j=1}^{N_q} w_{j,1} d_j^k c_{y,1}, \quad (19)$$

where in the above equations we applied a one-point quadrature approximation for the integration over the concentration coordinate, since the breakage and coalescence frequencies are considered weak functions of the solute concentration as will be pointed out below. Accordingly, the system of Eq. (18) describes the pure hydrodynamics of the LLEC coupled to the system of Eq. (19) through the mean solute concentration, which is given by the quadrature node, $c_{y,1}$, as follows:

$$c_{y,1} = C_y(t, z) = \frac{\int_0^\infty \int_0^{c_{y,\max}} c_y v(d) n_{d,c_y}(\psi) \partial d \partial c_y}{\int_0^\infty \int_0^{c_{y,\max}} v(d) n_{d,c_y}(\psi) \partial d \partial c_y} = \frac{\mu_{3,1}(t, z)}{\mu_{3,0}(t, z)}. \quad (20)$$

Note that the integration over the solute concentration in the above system of equations becomes entirely in terms

of the moments if the breakage and coalescence frequencies, the overall mass transfer coefficient, as well as the droplet rise velocity are solute concentration independent. In this work, a hybrid transformation is utilized by evaluating the concentration-dependent functions in Eqs. (8)–(15) using the value of $c_{y,1}$ from Eq. (20) so that these equations are written in terms of the marginal density, $q(d; t, z) = \int_0^{c_{y,\max}} c_y n_{d,c_y}(\psi) \partial c_y$. For example, Eq. (15) becomes

$$q_1(d; t, z) = \omega(d, d', \phi_y, \mathbf{P}|_{c_{y,1}}) q(d; t, z). \quad (21)$$

It is now clear that the knowledge of the $2N_q - 1$ moments, $\mu_{k,0}$ and $\mu_{k,1} = \int_0^\infty d^k q(d; t, z) \partial d = \sum_{j=1}^{N_q} w_j' d_j'^k$ is sufficient to evolve the weights and the abscissas (w, w', d and d') in time and space starting from a known initial state.

To find these weights and abscissas, we have used two approaches: the first one is through the use of the product difference (PD) algorithm as suggested by Gordon (1968) and recently described by Marchisio et al. (2003a,b); McGraw (1997). In this approach, the moment sequence is used to generate a well-conditioned, real and symmetric tridiagonal matrix, where its eigenvalues are the abscissas, and the weights are found from the square of the first element of its eigenvectors.

The second approach proceeds through reducing the index of the partial differential algebraic (PDAE) system above by differentiating Eqs. (18) and (19) with respect to time to get a system of PDEs in terms of the weights and abscissas (for more details about the index concept, the reader could refer to Martinson and Barton, 2000). However, writing the above system in terms of the weights and abscissas is rather lengthy and needs special treatment concerning the boundary and initial conditions and hence it will be presented separately.

In the present model, the breakage and coalescence frequencies, ω and Γ , respectively, are functions of the system physical properties. However, the dependence of the dispersed phase physical properties on the solute concentration is taken into account by evaluating them using the solute average concentration in the dispersed phase, rather than from the individual droplet concentration. This assumption is consistent with the QMOM, and at the same time it is reasonable since the breakage and coalescence frequencies are not strong functions of concentration (except the interfacial tension) (Gerstlauer, 1999).

Note that the system of moment equations above represents convective-diffusion partial differential equations, which proved to be dominated by convection (Attarakih et al., 2004a). This calls for specialized techniques to discretize the space variable, where it is proposed a couple of the recently published first- and second-order conservative numerical schemes to perform this task (Attarakih et al., 2004a).

4. Results and discussion

As mentioned in Section 1, we considered in this work a short segment of an RDC LLEC consisting of five compartments having over all dimensions: 0.15×0.15 m. To focus the work on the internal coordinate discretization, a four-compartment model is proposed, which consists of two feeding (for the dispersed and the continuous phases), one active, and upper settling compartments. The technical specifications of this column are reported by Simon et al. (2003).

For the numerical evaluation purposes of the BVQMOM, we also extended the GFP technique described by Attarakih et al. (2004a) to include mass transfer. The governing equations in this model are essentially the same as those described by the above BVQMOM. We adopted the same ideas described in Section 3 to split Eq. (1) into two systems in terms of the two densities: $q(d; t, z)$ and $n_d(d, ; t, z)$. The GFP technique is chosen to be internally consistent (see Section 1) with respect to droplet total number and volume. This technique is denoted in this work by GFPMT and will be reported separately in a subsequent publication. In all the numerical simulations, the inlet feed distribution is taken as a normal distribution fitted to the experimental data of Simon (2004) with droplet mean diameter of 2.1 mm and standard deviation of 0.5 mm. The two chemical systems used are those of the EFCE denoted by system 1 and system 2, where system 1 is water–acetone–toluene and system 2 is water–acetone–*n*-butyl acetate. The physical properties of these systems are available online (<http://www.dechema.de/Extraktion>). The individual mass transfer coefficients as predicted from the relations reported by Zhang et al. (1985) and Weinstein et al. (1998) are denoted as mass transfer model 1 and those of Kumar and Hartland (1999) are denoted as mass transfer model 2. The minimum and maximum droplet diameters used in the simulation are $d_{\min} = 0.025$ mm and $d_{\max} = 8$ mm such that a negligible number of droplets exist outside this range. For the GFPMT, the droplet diameter is discretized using a geometric grid with number of pivots, $M_x = 100$, and for the BVQMOM $N_q = 4$.

The desired integral properties of the dispersed phase are calculated from the available moments if they could be explicitly expressed in terms of them such as $\phi_y = \mu_{3,0}$, $d_{32} = \mu_{3,0}/\mu_{2,0}$. However, if the desired integral property could not be written directly in terms of the moments, the available quadrature weights and abscissas are used in the integration quadrature. The inlet solute concentrations in the continuous and dispersed phases are taken as 100 and 0 kg/m^3 , respectively, and the total flow rate of each phase is taken as $2.778 \times 10^{-5} \text{ m}^3/\text{s}$. The terminal droplet velocity is evaluated from the Vgines correlation for system 1 and from that of Klee and Treybal for system 2, based on the procedure described by Gourdon et al. (1994), with the slowing factor of Modes (2000). The resulting system of DAE was solved using the ordinary differential equation solver, ode45, of MATLAB software version 6.1 with toler-

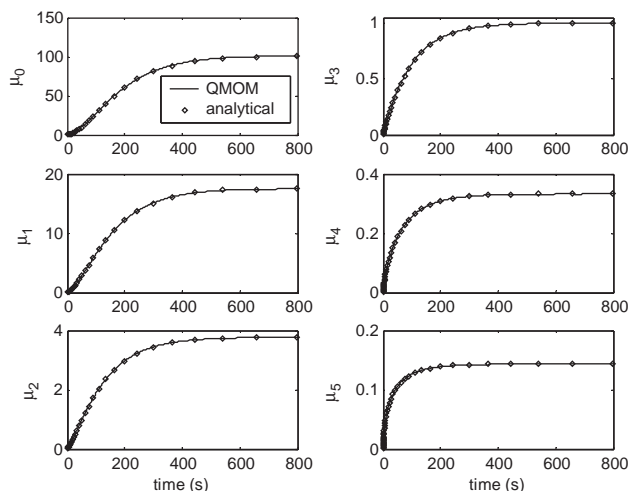


Fig. 1. Comparison between the analytical and numerical moments using the QMOM for droplet breakage in a CST with $\tau = 100$ s at a steady state. The analytical solution is given by Attarakih et al. (2004b).

ances: $RelTol = 10^{-6}$ and $AbsTol = 10^{-8}$ on Pentium III PC of 700 MHz speed.

Before we start our full numerical simulation of the present model, we want to gain some trust in the performance of the QMOM by comparing its prediction with some available analytical solutions. Recently, Attarakih et al. (2004b) derived the analytical solution of droplet breakage in a continuous flow vessel for $n_y^{\text{in}}(d) = 3d^2e^{-d^3}$, $\Gamma(d) = v(d)$, $\beta_n(d) = 6d^2/d'^3$ and zero initial condition. The time evolution of the first six moments is shown in Fig. 1, where excellent agreements between the predicted and the analytical solutions are evident. The difficulty of evolving the weights and abscissas from the zero initial condition was overcome by introducing a small lag time until the values of the moments exceed a certain specified tolerance. For this, the square root of the machine epsilon was found a good value for all the present simulations.

Fig. 2 (the left-hand side) shows the dynamic response of the dispersed phase hold-up and the Sauter droplet diameter (d_{32}) for pure breakage and pure coalescence (using the breakage and coalescence functions described in Sections 2.3.1 and 2.3.2) as predicted by the GFPMT and the BVQMOM. Three important aspects are evident in Fig. 2: First, the predicted ϕ_y and d_{32} are almost identical using both numerical methods over the whole simulation range. Second, pure droplet breakage produced higher values of the dispersed phase hold-up than the case of pure coalescence at the same energy input (250 rpm) as expected. Third, the droplet breakage increases with increase in energy input accompanied by a decrease in the Sauter droplet diameter.

Fig. 2 (the right-hand side) shows the solute concentration in the continuous (C_x) and dispersed (C_y) phases as a function of time. The good agreement between the predictions of the GFPMT and the QMOM is evident over the

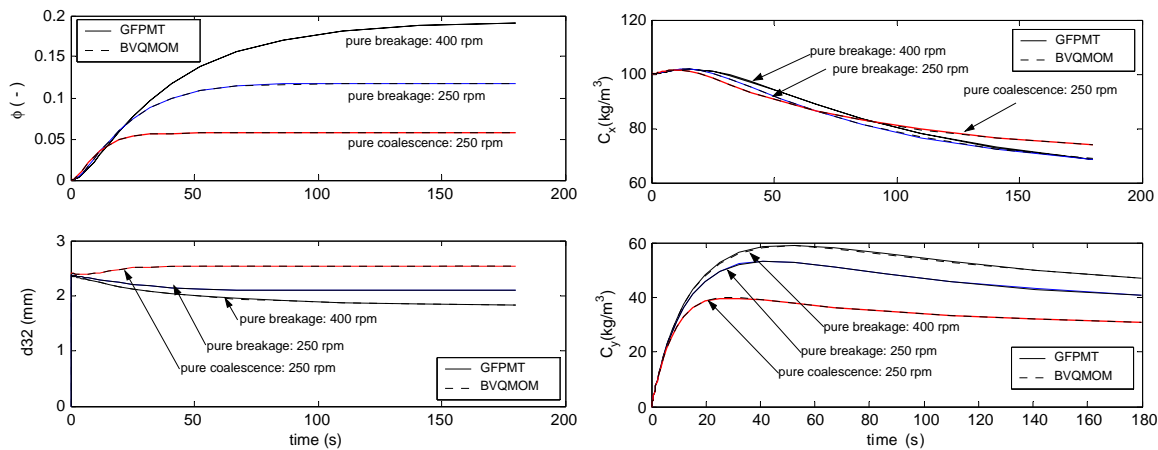


Fig. 2. The response of the dispersed phase hold-up, the d_{32} droplet diameter and the solute concentrations in both phases as predicted by the GFPMT and the BVQMOM using the chemical system 1.

whole simulation period. It is clear how the increasing rate of breakage increases the quantity of solute transferred to the dispersed phase by creating more small droplets and hence more interfacial area for the mass fluxes. Since the hold-up of the continuous phase is greater than that of the dispersed phase, the influence of the breakage and coalescence on the solute concentration in the continuous phase is not so great. One important aspect of this dynamic simulation is the slow response of the solute concentrations when compared to the dispersed phase hold-up. More interestingly, the response of the dispersed phase becomes slower as the droplet size (represented by d_{32}) decreases, indicating the slow motion of the small droplets.

Fig. 3a depicts the cumulative number densities using different droplet interaction mechanisms at different energy inputs as predicted by the GFPMT and the BVQMOM. It is clear that as the energy input increases, small-size droplet populations are produced, hence shifting the droplet spectrum to the left. On the other hand, the droplet coalescence produced populations of large droplets that are shifted to the right as expected (compare pure breakage and coalescence at 250 rpm). A more striking result is the good accuracy of the reconstructed solution using only the first four terms of the Laguerre polynomial weighted by the gamma function (Hulburt and Katz, 1964). Actually, this simple reconstruction technique is found more stable than that recommended by Diemer and Olson (2002). The latter is based on a modified gamma function and requires a multidimensional minimization technique to evaluate its parameters from the available moments. This fact is true not only for this case, but also for various droplet interaction mechanisms of available analytical solutions (coalescence with constant and sum frequencies, constant coalescence frequency plus growth, diffusion-controlled growth, sum coalescence frequency plus first-order removal, droplet breakage in continuous vessel) investigated by the authors. The good accuracy of this simple technique may be due to the cumulative nature

of the reconstructed distribution since the information carried by the moments (also the quadrature points) is accurate in estimating the integral quantities associated with the distribution. Anyhow, the approach deserves to be studied further.

Fig. 3b depicts the effect of the system physical properties on the extent of droplet breakage at a fixed energy input of 400 rpm. Since the system water–acetone–toluene has an equilibrium interfacial tension almost two times higher than that of the system water–acetone–*n*-butyl acetate, it is expected that the droplet populations of the second system will break up more easily than the first one based on the reasoning in Section 1. This fact is again emphasized in Fig. 3b by the higher value of the dispersed phase hold-up for the second system and the lower value of the Sauter diameter.

Fig. 4a depicts the hydrodynamic and solute concentrations responses using the two different mass transfer models described above. First, the two numerical schemes have almost the same predictions of all the responses, and second, the two mass transfer models produced almost identical results with little discrepancy in the dispersed phase solute concentration. It is clear that both the numerical methods are able to handle simple and sophisticated mass transfer expressions without any notable problems.

In Fig. 4b, we presented the covariance for the bivariate number density, $n_{d,c_y}(\psi)$, from the available moments as predicted by the BVQMOM to shed more light on the degree of association between the droplet diameter and solute concentration random variables. In the case of no mass transfer, the covariance is zero and there is no association between the droplet size and its concentration as expected. In the presence of mass transfer, the covariance is dependent on the prevailing interaction mechanism. The great association occurs when the droplet breakage is active alone, since this case leads to sharp distributions as is evident in Fig. 3a.

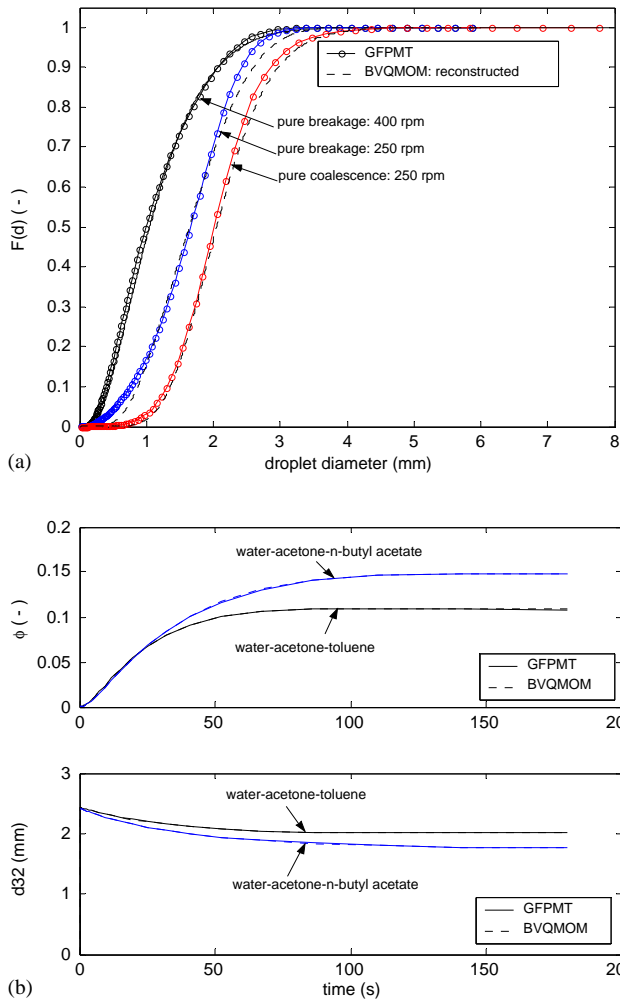


Fig. 3. (a) The predicted cumulative number densities using the GFPMT and the reconstructed (bases on Laguerre polynomials) ones at a steady state using the chemical system 1. (b) The response of the dispersed phase hold-up and the Sauter droplet diameter as predicted by the GFPMT and the BVQMOM for droplet breakage using the chemical systems 1 and 2.

However, in the case of droplet coalescence the degree of association is smaller due to the low coalescence rate. Not that the magnitude of the covariance is always less than zero in the presence of mass transfer, which means that small droplets are associated with large solute concentrations as expected. Moreover, since the value of the covariance is not zero (except for the trivial case of no mass transfer), we conclude that the two random variables, d and c_y , are not independent.

To get more insight into the accuracy and convergence characteristics of the GFPMT and the BVQMOM we carried out the steady state tests shown in Table 2. Concerning the GFPMT, it is clear that the error induced in the various integral quantities (d_{32} , ϕ_y , C_x , C_y) is less than 1% when the level of discretization is reduced from 120 to 50, accompanied by a significant reduction of the CPU time (from 1287 to 162 s).

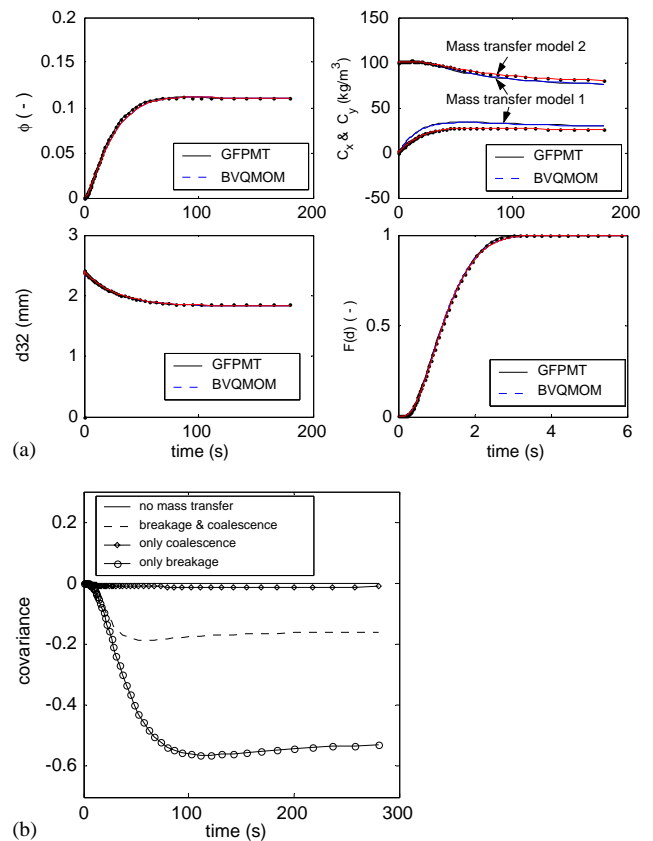


Fig. 4. (a) The effect of the mass transfer models (filled circles: model 2) on the response of the hold-up, Sauter droplet diameter, solute concentrations and the cumulative number density as predicted by the GFPMT and the BVQMOM for droplet breakage and coalescence using the chemical system 2. (b) The effect of the mass transfer and various droplet interaction mechanisms on the response of the covariance between droplet diameter and concentration as predicted by the BVQMOM using the chemical system 2 and the mass transfer model 1.

The same thing could be said about the BVQMOM, when the number of quadrature points is reduced from 4 to 2. It is interesting to note that the BVQMOM is less expensive, in terms of the CPU time, than the GFPMT only when the number of quadrature points is 2. This is might be attributed to two reasons: First, as the number of quadrature points increases, the number of moment equations also increases with a wide spectrum of time responses (see Fig. 1). This makes the time step selected by the time integrator very small and hence increases the CPU time. For example, the number of successful time steps taken by the integrator for the BVQMOM is 500, while that for the GFPMT is 400 when $N_q = 4$ and $M_x = 50$. We also observed that the number of failure steps taken by the BVQMOM is more than that of the GFPMT. Second, the size of the eigenvalue problem increases as the number of quadrature points increases, and hence increases the time for finding the eigenvalues by iterative methods.

Table 2

The convergence of the GFPMT and the BVQMOM at a steady state using the chemical system 2

	GFPMT			BVQMOM		
	$M_x = 50$	$M_x = 120$	% relative error	$N_q = 2$	$N_q = 4$	% relative error
N (rpm)	400	400		400	400	
d_{32} (mm)	1.846	1.836	0.545	1.856	1.836	1.089
ϕ_y (–)	0.110	0.110	0.000	0.110	0.110	0.000
C_x (kg/m ³)	73.816	73.921	0.142	73.959	73.920	0.053
C_y (kg/m ³)	28.797	28.618	0.625	28.411	28.618	0.723
CPU time(s)	162	1287		59	300	

5. Conclusions

- A comprehensive bivariate population balance model is developed to predict the behavior of the spatially distributed population balances for LLECs. This model couples the hydrodynamics and mass transfer through the breakage and coalescence frequencies.
- Two numerical approaches were based on the extension of the GFP technique previously formulated by the authors (Attarakih et al., 2004a), and the QMOM was extended to handle the bivariate population density required for the description of coupled hydrodynamics and mass transfer in typical LLECs. The BVQMOM is also reinforced by a simple reconstruction technique of the cumulative marginal densities based on a four-term Laguerre expansion with a gamma distribution as the weighing function.
- Both the GFPMT and the BVQMOM are found to converge as the number of pivots or quadrature points increases, however, at the expense of the computational cost. Although the required number of ODEs using the GFPMT is greater than that required by the BVQMOM, it is still competing the BVQMOM when an adaptive time integrator is used.
- From the standard numerical tests, it is clear that the GFPMT and the BVQMOM are capable of describing the hydrodynamics and mass transfer behaviors in LLECs when supplied with accurate droplet transport and interaction functions (breakage and coalescence frequencies).

Notation

A_c	column cross-sectional area, m ²
C, c	solute concentration, kg/m ³
d	droplet diameter, m
d_{32}	Sauter mean droplet diameter, m
D, D_m	molecular diffusion and axial dispersion coefficients, respectively, m ² /s
K_{oy}	overall mass transfer coefficient based on the dispersed phase, m/s
M_x, N_q	number of pivots (classes) in the GFPMT and quadrature points, respectively

$n_{d,c_y} \partial d \partial c_y$	the number of droplets with d and $c_y \in [d \pm \partial d] \times [c_y \pm \partial c_y]$ per unit volume of the contractor, 1/m ³
N	rotor speed, 1/s
\mathbf{P}	vector of physical properties [$\mu \rho \sigma$]
Q	continuous or dispersed phase flow rate, m ³ /s
t	time, s
u	velocity, m/s
v	droplet volume, m ³
w	quadrature weight
z	space coordinate, m

Greek letters

β_n	daughter droplet distribution, 1/m
Γ	breakage frequency, 1/s
μ	viscosity, Pa s, or distribution moment
ρ	density, kg/m ³
σ	interfacial tension, N/m
ϕ	phase hold-up, dimensionless
ψ	internal and external coordinates vector ($[d \ c_y \ zt]$)
ω	coalescence frequency, m ³ /s

Subscripts

r	relative velocity
x, y	continuous and dispersed phases, respectively

Superscripts

*	equilibrium
.	derivative with respect to time
in	inlet

Acknowledgements

The authors wish to thank the DFG and DAAD for supporting this work.

References

- Attarakih, M.M., Bart, H.-J., Faqir, N.M., 2004a. Numerical solution of the spatially distributed population balance equation describing the hydrodynamics of interacting liquid–liquid dispersions. *Chemical Engineering Science* 59, 2567–2592.
- Attarakih, M.M., Bart, H.-J., Faqir, N.M., 2004b. Solution of the droplet breakage equation for interacting liquid–liquid dispersions: a conservative discretization approach. *Chemical Engineering Science* 59, 2547–2565.
- Bart, H.-J., 2003. Reactive extraction in stirred columns: a review. *Chemical Engineering and Technology* 26, 723–731.
- Cauwenberg, V., Degreve, J., Slater, M.J., 1997. The interaction of solute transfer Contaminants and drop break-up in rotating disc contactors: part II. The coupling of mass transfer and breakage process via interfacial tension. *Canadian Journal of Chemical Engineering* 75, 1056–1066.
- Coulaloglou, C.A., Tavlarides, L.L., 1977. Description of interaction processes in agitated liquid–liquid dispersions. *Chemical Engineering Science* 32, 1289–1297.
- Diemer, R.B., Olsen, J.H., 2002. A moment methodology for coagulation and breakage problems: Part 3 — generalized daughter distributions. *Chemical Engineering Science* 57, 4187–4198.
- Gerstlauer, A., 1999. Herleitung und Reduktion populationsdynamischer Modelle am Beispiel der Flüssig-Flüssig-Extraktion. *Fortschritt-Berichte VDI Reihe 3*, 612.
- Gordon, R.G., 1968. Error bounds in equilibrium statistical mechanics. *Journal of Mathematical Physics* 9, 655–663.
- Gourdon, C., Casamatta, G., Muratet, G., 1994. Population balance based modeling of solvent extraction columns. In: Godfrey, J.C., Slater, M.J. (Eds.), *Liquid–liquid Extraction Equipment*. Wiley, New York, pp. 137–226.
- Hamilton, R.A., Curits, J.S., Ramkrishna, D., 2003. Beyond log-normal distributions: Hermite spectra for solving population balances. *A.I.Ch.E. Journal* 49, 2328–2343.
- Handlos, A.E., Baron, T., 1957. Mass and heat transfer from drops in liquid–liquid extraction. *A.I.Ch.E. Journal* 3, 127–136.
- Hulburt, H.M., Katz, S., 1964. Some problems in particle technology. *Chemical Engineering Science* 19, 555–574.
- Kostoglou, M., Karabelas, A.J., 1994. Evaluation of zero order methods for simulating particle coagulation. *Journal of Colloid and Interface Science* 163, 420–431.
- Kostoglou, M., Karabelas, A.J., 2002. An assessment of low-order methods for solving the breakage equation. *Powder Technology* 127, 116–127.
- Kumar, A., Hartland, S., 1999. Correlations for prediction of mass transfer coefficients in single drop systems and liquid–liquid extraction columns. *Transactions of the Institution of Chemical Engineers* 77, 372–384.
- Kumar, S., Ramkrishna, D., 1996. On the solution of population balance equations by discretization-I. A fixed pivot technique. *Chemical Engineering Science* 51, 1311–1332.
- Manninen, M., Taivassalo, V., Kallio, S., 1996. On the mixture model for multiphase flow, Technical Research Center of Finland, VTT Publications, ESPOO, Report No. 288.
- Marchisio, D.L., Pikturna, J.T., Fox, R.D., Vigil, R.D., Baressi, A.A., 2003a. Quadrature method of moments for population-balance equations. *A.I.Ch.E. Journal* 49, 1266–1276.
- Marchisio, D.L., Vigil, R.D., Fox, R.O., 2003b. Quadrature method of moments for aggregating-breakage processes. *Journal of Colloid and Interface Science* 258, 322–334.
- Martinson, W.S., Barton, A.P., 2000. A differentiation index for partial differential-algebraic equations. *SIAM Journal of Scientific Computing* 21, 2295–2315.
- McGraw, R., 1997. Description of aerosol dynamics by the quadrature method of moments. *Aerosol Science and Technology* 27, 255–265.
- McGraw, R., Wright, D.L., 2003. Chemically resolved aerosol dynamics for internal mixtures by the quadrature of moments. *Journal of Aerosol Science* 34, 189–209.
- Modes, G., 2000. Grundsatzliche Studie zur Populationsdynamik einer Extraktionskolonne auf Basis von Einzeltröpfchenuntersuchungen. Aachen: Shaker Verlag.
- Mohanty, S., 2000. Modeling of liquid–liquid extraction column: a review. *Review Engineering Science* 16, 199–248.
- Nicmanis, M., Hounslow, M.J., 1998. Finite-element methods for steady-state population balance equations. *A.I.Ch.E. Journal* 44, 2258–2272.
- Piskunov, V.N., Golubev, A.I., 2002. The generalized approximation method for modeling coagulation kinetics—part 1: justification and implementation of method. *Journal of Aerosol Science* 33, 51–63.
- Ramkrishna, D., 2000. *Population Balances: Theory and Applications to Particulate Systems in Engineering*. Academic Press, San Diego.
- Ribeiro, L.M., Regueiras, P.F.R., Guimaraes, M.M.L., Madureira, C.M.N., Cruz-Pinto, J.J.C., 1997. The dynamic behavior of liquid–liquid agitated dispersions II. Coupled hydrodynamics and mass transfer. *Computers in Chemical Engineering* 21, 543–558.
- Rosner, D.E., Pyykönen, J.J., 2002. Bivariate moment simulation of coagulating and sintering nanoparticles in flames. *A.I.Ch.E. Journal* 48, 476–491.
- Rosner, D.E., McGraw, R., Tandon, P., 2003. Multivariate population balances via moment and Monte Carlo simulation methods: an important sol reaction engineering bivariate, scavenging, and optical properties for populations of nonspherical suspended particles. *Industrial and Engineering Chemistry Research* 42, 2699–2711.
- Schmidt, S., Simon, M., Bart, H.-J., 2003. Tropfenpopulationsmodellierung-Einfluss von Stoffsystem und technischen Geometrien. *Chemie Ingenieur Technik* 75, 62–67.
- Simon, M., 2004. Koaleszenz von Tropfen und Tropfenschwärmen, Ph.D. Thesis, TU Kaiserslautern.
- Simon, M., Schmidt, S., Bart, H.-J., 2003. The droplet population balance model—estimation of breakage and coalescence. *Chemical Engineering and Technology* 26, 745–750.
- Weinstein, O., Semiat, R., Lewin, D.R., 1998. Modeling, simulation and control of liquid–liquid extraction columns. *Chemical Engineering Science* 53, 325–339.
- Wilburn, N.P., 1964. Mathematical determination of concentration profiles in two-phase continuous countercurrent extractors. *Industrial and Engineering Chemistry Research Fundamentals* 3, 189–195.
- Wright, D.L., McGraw, R., Rosner, D.E., 2001. Bivariate extension of the quadrature method of moments for modeling simultaneous coagulation and sintering of particle populations. *Journal of Colloid and Interface Science* 236, 242–251.
- Zhang, S.H., Yu, S.C., Zhou, Y.C., Su, Y.F., 1985. A model for liquid–liquid extraction column performance—the influence of drop size distribution on extraction efficiency. *Canadian Journal of Chemical Engineering* 63, 212–226.